CONSTRUCTION AND PARAMETER CALIBRATION OF A DISCRETE ELEMENT MODEL FOR SEED GINGER IN SOWING OPERATIONS
/
播种期生姜离散元模型构建与参数标定

Jinbiao ZHANG[1], Jin CHENG*[1], Lin LIU[1], Jialin HOU[1], Rui HOU[2], Qiwei ZHAO[3], Yuhua LI[1]
[1] Shandong Agricultural University, Tai'an / China;
[2] Beijing University of Posts and Telecommunications, Beijing / China
[3] Dezhou Chunming Agricultural Machinery Company Limited, Dezhou / China
Cheng Jin, Tel: +8615666763312; Email: ttcheng@163.com

DOI: https://doi.org/10.35633/inmateh-79-87

Keywords: *discrete element method, seed ginger, particle interaction, angle of repose, DEM parameter calibration*

ABSTRACT
To address the lack of contact parameters for seed ginger and the insufficient accuracy of existing discrete element models used in simulations of seed ginger machinery, a discrete element modeling and contact parameter calibration method for irregularly shaped seed ginger was proposed. A discrete element model of seed ginger was constructed using 3D laser scanning and an adaptive multi-sphere filling method. The contact parameters between seed ginger and steel were calibrated using free-fall collision tests, inclined-plane tests, and combined inclined-plane–horizontal-plane tests. Using the angle of repose as the response variable, the optimal parameter combination was determined through steepest ascent tests and response surface methodology. The relative error between the simulated angle of repose and the value measured in the bench test was 2.24%. The results provide a modeling basis for the optimization and design of key components of seed ginger machinery and for investigating the dynamic interaction mechanisms among seed ginger particles.

摘要
针对生姜播种机械仿真研究中姜种接触参数缺失、模型精度不足的问题，提出一种不规则姜种的离散元建模与接触参数标定方法。基于三维激光扫描与多球自适应填充方法构建姜种离散元模型；采用自由落体碰撞法、斜面法及斜面-平面组合法标定姜种与钢材间接触参数；并以休止角为响应指标，结合最陡爬坡试验与响应面试验，获得最优参数组合，仿真休止角与台架试验实测值的相对误差为 2.24 %。研究结果可为生姜播种机械关键部件优化设计及颗粒群动态互作机理研究提供模型基础。

INTRODUCTION
Ginger is a vital specialty vegetable and medicinal crop in China, ranking first globally in both planting area and total yield, with stable and continuously growing market demand. Currently, ginger sowing operations face challenges such as labor shortages and low efficiency *(Yang et al., 2022)*. The irregular shape of seed ginger and their distinctive features like surface protrusions and nodes impose stringent requirements on single-seed picking and bud orientation during mechanized sowing. However, establishing a granular simulation model using the discrete element method enables precise analysis of microscopic force interactions, providing a crucial tool for the design verification and simulation optimization of key components in ginger sowing machinery *(Zhao et al., 2025)*. Accurate calibration of seed ginger-related contact parameters and the construction of discrete element models have become essential foundations for ensuring the rational design of core sowing machinery components and the accuracy of virtual simulations.

Currently, numerous researchers have conducted studies on the construction and parameter calibration of discrete element models for conventional crops. *Lu et al., (2023),* and others simulated the natural stacking and sowing processes of wheat seeds, effectively addressing the challenge of balancing simulation accuracy and computational time in the multi-sphere method. *Shi Linrong et al., (2018)* employed the slice modeling method to construct a potato seed model and validated the effectiveness of the stacking angle simulation parameters through physical experiments. *Lu Qi et al., (2023),* and others developed a soil-seed interaction model, determining contact parameter values using the response surface method.

---

[1] *Zhang Jinbiao[1], Ph.D. Stud.; Cheng Jin,* Ph.D.; Liu Lin, Ph.D.; Hou Jialin, Prof. Ph.D.; Hou Rui, Ph.D.; Zhou Qiwei.; Li Yuhua, Ph.D.*

Xia Junfang et al., (2024), *Liao Yitao et al., (2020)*, and *Shi Ruijie et al., (2022),* combined simulation with bench tests to accurately obtain contact parameters for rice straw, rapeseed stems, and sesame stems, providing foundational data for low-loss harvesting technologies. Other scholars have also conducted relevant research on the establishment of discrete element simulation model and parameter calibration of crops and products such as alfalfa (*Chen et al., 2023*), sunflower (*Guo et al., 2025*), tea (*Du et al., 2025*), quinoa (*Liu et al., 2020*), maize (*Jia et al., 2020*), coated cotton-seeds (*Wang et al., 2021*), sweet sorghum seeds (*Yang et al., 2026*) and millet threshing mixtures (*Huang et al., 2026*). These studies predominantly employed a combination of physical experiments and simulation to optimize parameters but primarily focused on regular-shaped, single-mechanical-property agricultural granular materials. Under external loading, seed ginger exhibits dynamic mechanical responses, including friction and collision, as well as asymmetric stacking behavior characterized by the angle of repose, which differ fundamentally from those of conventional crop materials.

To address the complex stacking behavior caused by the irregular shape of seed ginger, a parameter calibration optimization procedure was established based on steepest ascent tests and response surface methodology, providing a calibration approach suitable for irregular block-shaped seed materials. This study systematically reports key physical and mechanical properties of seed ginger during sowing, addressing a gap in the existing research and providing an accurate modeling basis for further investigation of dynamic interaction mechanisms in mechanical ginger sowing and for the optimized design of key components.

MATERIALS AND METHODS

Determination of physical properties of seed ginger

In order to obtain the basic physical characteristic parameters of seed ginger, this study selected "Laiwu Big Ginger" with intact scales after germination as the experimental object. This variety has strong growth potential and a yield of about 30 t/hm^2. It is the main cultivated variety in Shandong region and has certain representativeness. Regarding the shape of seed ginger Based on the principle of "moderate block size, typical shape, and full scale", seed ginger were randomly spread out on the open space due to their complex and irregular characteristics. Then, the five point sampling method (Fig.1) was used, with 40 seed ginger randomly taken from each sampling point, for a total of 200 seed ginger as the measurement samples. Using the AES-G5 electronic scale, the average mass of the sample monomer was 68.5 g. The volume was measured using the drainage method, and the average density of the seed ginger was calculated to be 1094.7 kg/m^3. The average moisture content of the seed ginger was determined to be 64.38% using the standard drying method. The external dimensional parameters of seed ginger were measured and statistically analyzed using a vernier caliper with an accuracy of 0.1 mm. Considering the typical irregular block structure of seed ginger, this study selected the maximum radial size of the main body of seed ginger at the thick end and the minimum radial size at the thin end as the external dimensional parameter indicators. The results are shown in Table 1.

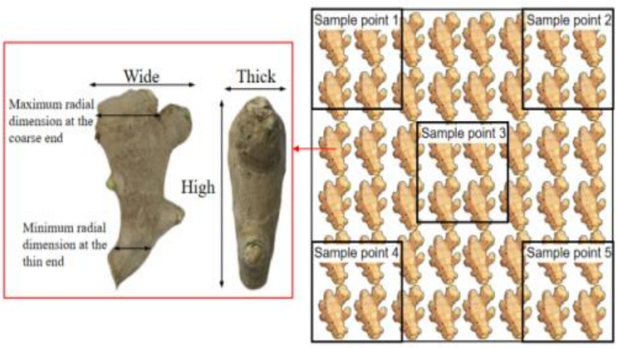

Fig. 1 - Five point sampling method

Table 1

Measurement results of external dimensions parameters of seed ginger during sowing period

Project	High[mm]	Width[mm]	Thickness [mm]	Maximum radial dimension at the coarse end[mm]	Minimum radial dimension at the thin end[mm]
Max	125.2	74.3	35.6	42.5	17.8
Min	72.7	52.6	24.9	35.4	12.4
Mean	93.8	63.7	31.7	37.8	14.7
Standard Deviation	13.7	9.3	5.8	2.9	3.1

The Poisson's ratio, elastic modulus, and shear modulus of seed ginger were determined through compression tests *(Sun et al., 2025)*. Cylindrical pulp specimens with a diameter of 10 mm and a length of 20 mm were prepared and placed on the lower compression platen of a TA-XT2i texture analyzer. The pre-compression speed of the upper platen was set to 60 mm/min, the compression speed to 5 mm/min, and the compression distance to 5 mm. Ten replicate compression tests were conducted. The radial dimensions of the specimens before and after compression were measured, and the mean Poisson's ratio μ of seed ginger was calculated using Eq. (1) as 0.46. Compression was then continued until the cylindrical specimen completely collapsed. The test was repeated ten times, and the maximum load *F* within the elastic deformation stage and the corresponding axial deformation ΔL were recorded. According to Eq. (2), the mean elastic modulus E of seed ginger was calculated as 2.97 MPa, as shown in Table 2. The shear modulus G was subsequently calculated using Eq. (3), yielding a mean value of 1.02 MPa.

$$\mu = \left|\frac{\varepsilon_t}{\varepsilon_a}\right| = \frac{\Delta d / d}{\Delta h / h} = \frac{\Delta dh}{\Delta hd} \tag{1}$$

$$E = \frac{Fh}{S\Delta L} \tag{2}$$

$$G = \frac{E}{2(1+\mu)} \tag{3}$$

where: μ is Poisson's ratio; ε_t is the radial deformation of the sample, [mm]; ε_a is the axial deformation of the sample, [mm]; Δd is the radial size change, [mm]; d is the radial original size, [mm]; Δh is the axial size change, [mm]; h is the axial original size, [mm]. E is the elastic modulus, [MPa]; F is the maximum load during the elastic stage, [N]; S is the compressive cross-sectional area, [mm^2]; ΔL is the compression deformation of the sample at the maximum load, [mm]; G is the shear modulus, [MPa].

Table 2

Determination results of compression test of seed ginger during sowing period

No.	Radial dimension after compression [mm]	variation[mm]	Poisson's ratio	maximum load/ [N]	Compression deformation amount [mm]	Elastic Modulus
1	11.05	1.05	0.42	92.10	8.20	2.86
2	11.13	1.13	0.45	94.92	8.25	2.93
3	11.20	1.20	0.48	97.46	8.30	2.99
4	11.25	1.25	0.50	100.94	8.40	3.06
5	11.00	1.00	0.40	92.49	8.15	2.89
6	11.23	1.23	0.49	97.39	8.35	2.97
7	11.15	1.15	0.46	98.52	8.28	3.03
8	11.28	1.28	0.51	93.93	8.22	2.91
9	11.08	1.08	0.43	102.54	8.45	3.09
10	11.18	1.18	0.47	97.04	8.32	2.97
Max	11.28	1.28	0.51	102.54	8.45	3.09
Min	11.00	1.00	0.40	92.10	8.15	2.86
Mean	11.16	1.16	0.46	96.73	8.29	2.97
Standard Deviation	0.09	0.09	0.036	3.44	0.09	0.075

Compare and analyze the mechanical properties of seed ginger with typical agricultural bulk materials *(Zhou et al., 2023; Cai et al., 2024; Zhang et al., 2025; Zhang et al., 2022)*, as shown in Table 3. Compared with high-stiffness particles such as wheat and beans, seed ginger exhibits markedly lower stiffness. Compared with root and tuber crops such as potatoes, water chestnuts, yams, and sweet potatoes, seed ginger has a higher Poisson's ratio.

The typical low stiffness and high deformation physical characteristics of ginger provide a reliable theoretical basis for the selection and parameter configuration of low stiffness contact models in subsequent discrete element simulations, which result in high viscous resistance and asymmetric contact phenomena during dynamic collisions and natural accumulation processes.

Table 3

Comparison of mechanical properties of typical agricultural bulk materials

Name	Wheat	Soybean	Potato	Water Chestnut	Yam	Sweet Potato	Ginger
Type	Cereals	Legumes	Roots and Tubers	Roots and Tubers	Roots and Tubers	Roots and Tubers	Roots and Tubers
Elastic Modulus	37	180	5.65	5.433	3.92	3.22	2.97
Poisson's Ratio	0.30	0.40	0.42	0.395	0.4	0.28	0.46

Construction of Discrete Element Model

During the sowing period, seed ginger exhibit a significant irregular block structure, and it is difficult to accurately reflect their complex boundary contours using conventional single sphere or ellipsoid models. The multi-sphere adaptive filling model can flexibly approach the irregular block structure and angle characteristics by adjusting the number, radius and spatial arrangement of the constituent spheres, and also simplify the contact between particles with complex shapes as the interaction between spheres. This study utilized a high-precision 3D laser scanner (Accuracy: 0.02 mm; Resolution: 0.02 mm; Scanning speed: 2,800,000 points/s) to obtain 3D point cloud data on the surface of ginger samples, and imported it into Geomagic Studio software for reverse engineering processing. During the processing, the focus is on preserving the coarse and fine end contour features of seed ginger, and then using HyperMesh software for mesh partitioning and optimization to export high-precision 3D geometric models of seed ginger. The three-dimensional model was imported into EDEM software. Based on the multi-sphere combination method, a small ball with a radius of 2 mm was selected to discretize and fill the model. The smoothing value was set to 3, and the total number of spheres was 6988. The discrete element model of ginger seeds was constructed (Fig. 2).

Seed ginger is a kind of granular material with large size, and the particles will not adhere and agglomerate with each other due to the effect of water and chemical substances, the measured mechanical parameters of seed ginger were directly assigned in EDEM software, and the Hertz Mindlin (no slip) contact model was selected. This setting accurately reproduces the high viscosity resistance and asymmetric stacking behavior of seed ginger, laying the foundation for precise calibration of subsequent contact parameters.

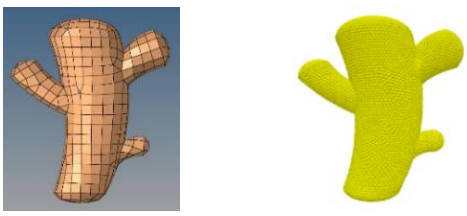

Fig. 2 - Seed ginger simulation model

Coefficient of restitution between seed ginger and steel

The coefficient of restitution is a dimensionless parameter that characterizes the ability of two colliding bodies to recover kinetic energy after impact *(Guo et al., 2023)*. In this study, the coefficient of restitution between seed ginger and a steel plate was measured using a free-fall collision test. A smooth steel plate was fixed horizontally on the base, and 30 seed ginger samples were randomly selected and released from rest from a vertical height of 200 mm. After impact with the steel plate, the samples rebounded. A 1 mm grid was placed in the background as a reference scale, and the rebound process was analyzed frame by frame using a high-speed camera. The mean maximum rebound height h_r was 38.6 mm. According to Eq. (4), the coefficient of restitution *e* between seed ginger and steel was calculated as 0.439. A corresponding simulation model was established in EDEM. The particle factory generated seed ginger particles with zero initial velocity, and the seed ginger–steel coefficient of restitution was set to 0.439. The particles were allowed to fall freely under gravity and collide with the steel plate. The simulation data storage interval was 0.01 s, the total simulation time was 20 s, and the time step was 4.501 × 10^{-7} s. Considering both computational accuracy and efficiency, the minimum fluid-grid porosity setting was specified such that the grid size was three times the particle diameter. The center-of-mass trajectories of the seed ginger particles were tracked using the post-processing tools. The mean maximum rebound height after impact was 34.9 mm, corresponding to a simulated coefficient of restitution of 0.418.

The relative error between the simulated coefficient of restitution and the bench-test value of 0.439 was 4.78%, indicating that the established discrete element model of seed ginger could adequately reproduce the actual collision characteristics. Therefore, the coefficient of restitution *e* between seed ginger and the steel plate was set to 0.439. The experimental setup and simulation process are shown in Fig. 3.

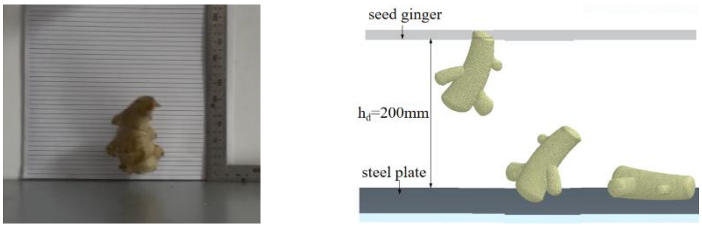

Fig. 3 - Calibration test for the coefficient of restitution between seed ginger and steel

$$e = \sqrt{\frac{h_r}{h_d}} \tag{4}$$

where: e is the coefficient of restitution; h_r is the maximum rebound height of the seed ginger, [mm].

Sliding friction coefficient between ginger and steel

The sliding friction coefficient between seed ginger and a steel plate was measured using the inclined-plane method *(Jiang et al., 2023)*. The longitudinal axis of the seed ginger was aligned parallel to the long side of the steel plate. A digital inclinometer was attached to one side of the plate, and one end of the plate was raised slowly and uniformly to increase the inclination angle. When the seed ginger was on the verge of sliding, the inclination angle was recorded as the critical sliding angle α_1. The test was repeated 30 times, yielding a mean critical sliding angle of 25.75°. According to Eq. (5), the sliding friction coefficient f_1 between seed ginger and the steel plate was calculated as 0.482. For simulation validation, the sliding friction coefficient between the discrete element model of seed ginger and the steel plate model was set to 0.482. A simulation model corresponding to the bench test was established, and the inclination angle of the plate was gradually increased until the seed ginger model began to slide. The critical sliding angle obtained from the simulation was 24.90°, corresponding to a simulated sliding friction coefficient of 0.464. The relative error between the simulated and experimentally measured values was 3.73%, indicating good agreement. Therefore, the sliding friction coefficient f_1 between seed ginger and the steel plate was set to 0.482. The bench-test and simulation procedures are shown in Fig. 4.

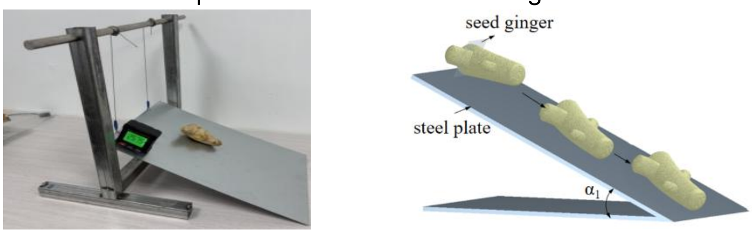

Fig. 4 - Calibration test for the sliding friction coefficient between seed ginger and steel

$$f_1 = \tan\alpha_1 \tag{5}$$

Rolling friction coefficient between seed ginger and steel

In this study, the rolling friction coefficient between seed ginger and steel was measured using a combined inclined-plane and horizontal-plane method. The seed ginger was placed on a steel plate inclined at an angle α_2 of 45°, with its longitudinal axis aligned with the long side of the plate, and was released from rest at a vertical height N of 200 mm above the horizontal plane. The seed ginger accelerated while rolling down the inclined plate and then transitioned smoothly onto the horizontal steel plate, where it decelerated under the action of rolling friction until coming to rest. The test was repeated 30 times, and the mean rolling distance M on the horizontal plate was 178 mm. According to Eqs. (6) and (7), the rolling friction coefficient f_2 between seed ginger and the steel plate was calculated as 0.308. A simulation model with the same dimensions was established in EDEM. The calibrated coefficient of restitution and sliding friction coefficient, together with the rolling friction coefficient to be validated, were assigned to the seed ginger particle model. A seed ginger particle with zero initial velocity was generated at a height of 200 mm. After 30 simulation runs, the mean horizontal rolling distance was 192 mm, corresponding to a simulated rolling friction coefficient of 0.324. The relative error between the simulated and experimentally measured values was 5.19%, indicating good agreement and supporting the validity of the calibrated parameter. Therefore, the rolling friction coefficient f_2 between seed ginger and the steel plate was set to 0.308. The bench-test and simulation procedures are shown in Fig. 5.

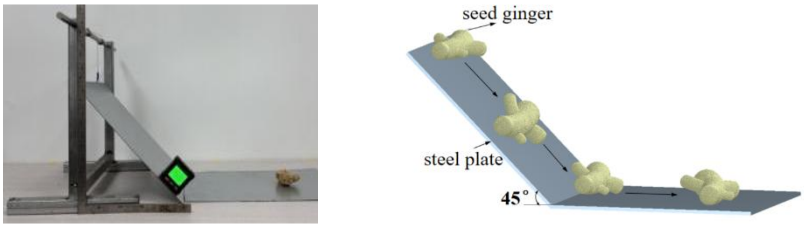

Fig. 5 - Calibration test for the rolling friction coefficient between seed ginger and steel

$$f_2\left(B+M\cos\alpha_2\right)=M\sin\alpha_2 \tag{6}$$

$$B=\frac{N}{\sin\alpha_2} \tag{7}$$

where: α_2 is the inclination angle of the steel plate, [°]; B is the rolling distance of the seed ginger along the inclined plane, [mm]; M is the horizontal rolling distance of the seed ginger, [mm].

Calibration of contact parameters between seed ginger particles

Given the complex and irregular shape of seed ginger, it is difficult to ensure the accuracy of directly measuring seed ginger–seed ginger contact parameters using bench tests alone. The angle of repose can reflect the combined effects of interparticle friction, collision, and asymmetric accumulation behavior. In this study, the experimentally measured angle of repose was used as the target response value. Based on the parameter ranges determined from the bench tests, the seed ginger–seed ginger coefficient of restitution, sliding friction coefficient, and rolling friction coefficient were selected as the experimental factors, and a three-factor, three-level orthogonal test was conducted to determine the optimal combination of contact parameters.

To determine the range of the seed ginger–seed ginger coefficient of restitution, a double-inclined-plane collision method was used *(Xia et al., 2019)*, as illustrated in Fig. 7. Two inclined planes, each set at an inclination angle of 45°, were fixed on the test bench. Seed ginger slices were closely arranged over the working surfaces of the inclined planes to form seed ginger–seed ginger collision layers. The vertical heights from the collision points on the two inclined planes to the horizontal plane were set to H_1 = 200 mm and H_2 = 500 mm, respectively. An intact seed ginger sample was released from rest from a vertical height K of 200 mm above the impact point on the inclined plane. After collision, the sample was projected from the inclined plane and eventually landed on a horizontal plane covered with coordinate paper. The corresponding horizontal travel distances Z_1 and Z_2 were recorded. The test was repeated 30 times, and the seed ginger–seed ginger coefficient of restitution e_1 was calculated using Eqs. (8)–(10). The preliminary range of e_1 was determined to be 0.15–0.65.

$$e_1=\frac{2\sqrt{V_X^2+V_Y^2}\cdot\cos\left[45^\circ+\arctan\left(\frac{V_Y}{V_X}\right)\right]}{\sqrt{0.8g}} \tag{8}$$

$$V_X=\sqrt{\frac{gZ_1Z_2\left(Z_1-Z_2\right)}{\left(0.4Z_2-Z_1\right)}} \tag{9}$$

$$V_Y=\frac{0.5V_X}{Z_2}-\frac{gZ_2}{2V_X} \tag{10}$$

where: Z_1 is the horizontal landing distance corresponding to the first inclined plane, [m]; Z_2 is the horizontal landing distance corresponding to the second inclined plane, [m]; V_X is the horizontal velocity component after collision with the inclined plane, [m/s]; V_Y is the vertical velocity component after collision with the inclined plane, [m/s]; g is the acceleration due to gravity, [m/s^2].

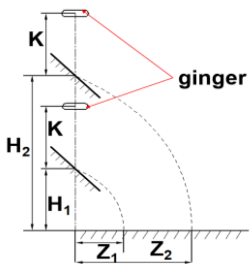

Fig. 6 - Schematic diagram of the bench test for measuring the coefficient of restitution between seed ginger samples

Sliding and rolling friction coefficients between seed ginger samples

In this study, a modified inclined-plane method and a combined inclined-plane and horizontal-plane method were used to determine the preliminary ranges of the seed ginger–seed ginger sliding and rolling friction coefficients. A representative seed ginger sample was cut longitudinally, and the cut pieces were closely arranged and fixed onto the surface of a steel plate to form a seed ginger friction surface. During the sliding test, an intact seed ginger sample was placed on the friction surface as the sliding body, with its longitudinal axis aligned parallel to that of the seed ginger pieces fixed to the plate. One end of the friction plate was raised slowly and uniformly, and the critical inclination angle at the onset of macroscopic sliding was recorded. Thirty seed ginger samples were tested, and the seed ginger–seed ginger sliding friction coefficient f_3 was calculated using Eq. (5), yielding a range of 0.37–0.87. For the rolling friction test, the inclination angle was fixed at 45°. A seed ginger sample was positioned at a vertical height D of 200 mm above the horizontal plane, with its transverse orientation perpendicular to the longitudinal direction of the seed ginger pieces on the friction surface. The sample rolled to the end of the inclined plate along an approximately curved trajectory and subsequently landed on the contact surface. The horizontal distance to the first landing point, Z_3, was recorded. Thirty seed ginger samples were tested, and the seed ginger–seed ginger rolling friction coefficient f_4 was calculated using Eq. (11), yielding a range of 0.32–0.82. The bench-test procedures are shown in Fig. 7.

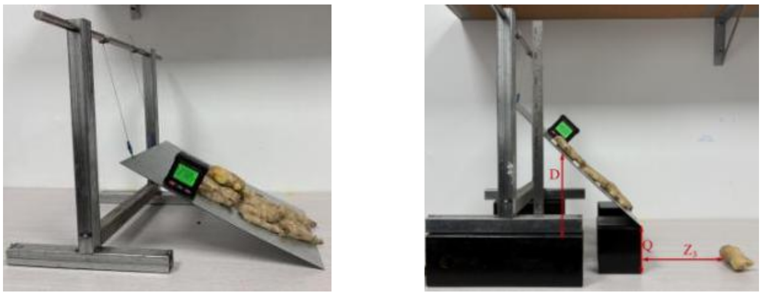

Fig. 7 - Bench tests for the sliding and rolling friction coefficients between seed ginger samples

$$f_4 = \frac{D - Z_3^{\ 2}}{2(Q - Z_3)D} \tag{11}$$

where: Z_3 is the horizontal distance to the first landing point on the contact surface, [mm]; Q is the vertical height difference between the end of the inclined plate and the contact surface, [mm].

Physical angle of repose test

In this study, the bottomless-cylinder lifting method (*Zhang et al., 2022*) was used to determine the physical angle of repose of seed ginger. A cylindrical steel container with an inner diameter of 300 mm and a height of 900 mm was used for the test. Its relatively large diameter-to-height ratio helped reduce boundary effects during particle accumulation. Seed ginger samples were naturally filled into the cylinder, after which the cylinder was lifted vertically at a constant speed. Under gravity, the seed ginger mass collapsed and eventually formed a stable asymmetric pile. The angle between the natural slope of the pile and the horizontal surface was measured as the natural angle of repose θ of seed ginger.

To reduce errors associated with manual measurement, image processing was used to determine the angle of repose. After a frontal image of the pile was acquired, grayscale conversion and binarization were sequentially performed using a Python-based image-processing procedure, and the edge contour points were extracted from the binary image. The contour on one side of the pile was then fitted linearly using the least-squares method to obtain the slope of the fitted line, as shown in Fig. 8. After 30 repeated tests, the angle of repose θ of seed ginger was calculated using Eq. (12) as 28.60°.

Fig. 8 - Image-processing procedure for determining the angle of repose of seed ginger

$$\theta = \frac{180 \arctan T}{\pi} \tag{12}$$

Simulated angle of repose test and steepest ascent test

To obtain accurate values of the contact parameters between seed ginger particles, the angle of repose was used as the evaluation index, while the seed ginger-seed ginger coefficient of restitution, sliding friction coefficient, and rolling friction coefficient were selected as the experimental factors. A three-factor, three-level orthogonal test was conducted using EDEM simulations.

To further determine the optimal ranges and center levels of the experimental factors, a steepest ascent test was conducted based on the preliminary ranges of the seed ginger–seed ginger coefficient of restitution e_1 (0.15~0.65), sliding friction coefficient f_3 (0.37~0.87), and rolling friction coefficient f_4 (0.32~0.82). An EDEM simulation model consistent with the dimensions of the physical test setup was established. The particle factory generated seed ginger particles until the steel cylinder was filled, after which the cylinder was lifted vertically at a constant speed of 1 m/s. Under gravity, the seed ginger particles fell and accumulated on the contact surface beneath the cylinder. After the particle pile stabilized, the image-processing method described above was used to determine the simulated angle of repose θ_1. The relative error σ between the simulated and experimentally measured angles of repose was then calculated. Based on the steepest ascent test results, the coded levels of each factor for the subsequent three-factor, three-level orthogonal test were determined, as shown in Table 5.

Table 5

Results of the steepest ascent test and factor levels for the orthogonal design

No.	e_1	f_3	f_4	θ_1/[°]	σ/[%]	Coded level
1	0.15	0.37	0.32	29.94	4.69	/
2	0.25	0.47	0.42	29.69	3.81	-1
3	0.35	0.57	0.52	29.42	2.87	0
4	0.45	0.67	0.62	29.60	3.50	1
5	0.55	0.77	0.72	30.54	6.78	/
6	0.65	0.87	0.82	31.09	8.71	/

Response surface regression analysis and parameter optimization

Using the simulated angle of repose as the response variable, a Box–Behnken design was conducted. The experimental design and results are presented in Table 6. Multiple regression analysis was performed on the test data using Design-Expert software, and the corresponding analysis of variance and model reliability results are presented in Tables 7 and 8, respectively. A quadratic polynomial regression model for the simulated angle of repose θ_1 was established, as expressed in Eq. (13).

$$\theta_1 = 29.44 - 0.143e_1 + 1.84f_3 + 0.471f_4 + 0.118e_1f_4 - 0.3f_3f_4 + 0.124e_1^2 - 0.379f_3^2 \tag{13}$$

Table 6

Experimental design and results

No.	1	2	3	4	5	6	7	8	9	10	11	12	13	14	15	16	17
e_1	0.35	0.45	0.35	0.35	0.45	0.35	0.35	0.35	0.45	0.35	0.25	0.25	0.25	0.35	0.45	0.35	0.25
f_3	0.57	0.47	0.47	0.57	0.57	0.47	0.67	0.67	0.67	0.57	0.67	0.57	0.47	0.57	0.57	0.57	0.57
f_4	0.52	0.52	0.42	0.52	0.42	0.62	0.62	0.42	0.52	0.52	0.52	0.42	0.52	0.52	0.62	0.52	0.62
θ1/[°]	29.38	27.25	26.42	29.52	28.92	28.04	31.25	30.83	30.89	29.47	31.02	29.49	27.59	29.45	30.02	29.39	30.12
σ/[%]	2.72	4.72	7.62	3.22	1.12	1.96	9.27	7.80	8.01	3.04	8.46	3.11	3.53	2.97	4.97	2.76	5.31

Table 7

ANOVA for the quadratic regression model

Source	Model	e_1	f_3	f_4	e_1f_3	e_1f_4	f_3f_4	e_1^2	f_3^2	f_4^2	Residual	Lack of Fit	Pure Error	Cor Total
Sum of squares	30.00	0.1624	26.97	1.78	0.0110	0.0552	0.3600	0.0647	0.6032	0.0215	0.0683	0.0548	0.0135	30.07

Source	Model	e_1	f_3	f_4	e_1f_3	e_1f_4	f_3f_4	e_1^2	f_3^2	f_4^2	Residual	Lack of Fit	Pure Error	Cor Total
Degrees of freedom	9	1	1	1	1	1	1	1	1	1	7	3	4	16
Mean square	3.33	0.1624	26.97	1.78	0.0110	0.0552	0.3600	0.0647	0.6032	0.0215	0.0098	0.0183	0.0034	
F-value	341.64	16.65	2764.39	182.07	1.13	5.66	36.89	6.63	61.82	2.21		5.42		
P-value	<0.0001	0.0047	<0.0001	<0.0001	0.3231	0.0490	0.0005	0.0367	0.0001	0.1811		0.0680		

Table 8

Reliability analysis of the regression model

Response	R²	Adjusted R²	Predicted R²	Adeq Precision
θ_1	0.997	0.994	0.970	60.9143

The interaction response surfaces derived from the quadratic regression model are shown in Fig. 9. From the perspective of particle dynamics, the highly irregular morphology and high viscosity of seed ginger mean that increases in the sliding friction coefficient and rolling friction coefficient significantly enhance the interlayer shear resistance during particle accumulation, which is macroscopically reflected by a marked increase in the angle of repose. In contrast, the effect of the coefficient of restitution, which is mainly governed by the low-stiffness characteristics of seed ginger, on the static stacking morphology is relatively weak.

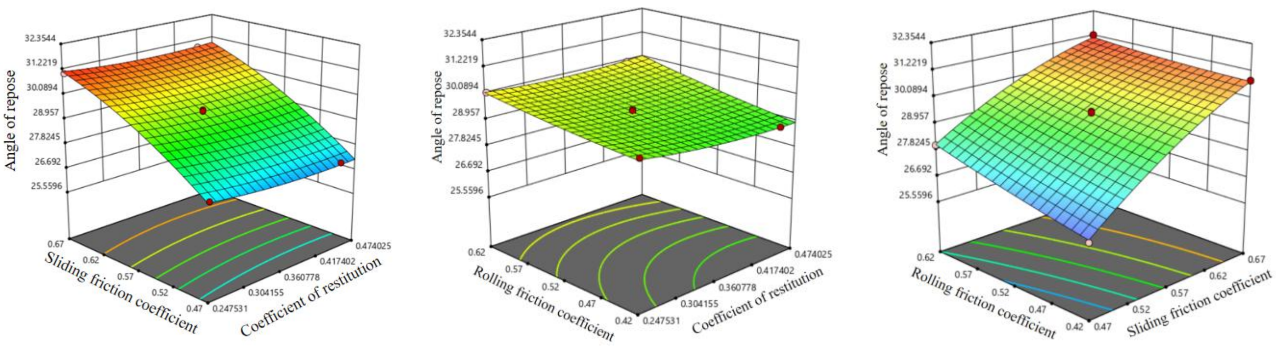

Fig. 9 - Interaction response surfaces of the particle contact parameters

RESULTS

Simulation validation

To determine the optimal solution of the quadratic regression model, multi-objective optimization of the influencing factors was performed using the Numerical module in Design-Expert, with the experimentally measured angle of repose of 28.60° specified as the target value.

The constraint system is given in Eq. (14). The optimized seed ginger–seed ginger contact parameters were a coefficient of restitution e_1 of 0.416, a sliding friction coefficient f_3 of 0.549, and a rolling friction coefficient f_4 of 0.450.

$$\begin{cases} \theta_1 = 28.60° \\ s.t. \begin{cases} 0.25 \le e_1 \le 0.45 \\ 0.47 \le f_3 \le 0.67 \\ 0.42 \le f_4 \le 0.62 \end{cases} \end{cases} \tag{14}$$

The optimal parameter combination was then introduced into EDEM for validation. The simulated angle of repose was 29.24° (Fig. 10), corresponding to a relative error of 2.24% compared with the experimentally measured value of 28.60°. The close agreement between the simulated and experimental results indicates that the discrete element model of low-stiffness seed ginger and the calibrated contact parameters can reliably reproduce its stacking behavior.

Fig.10 - Simulation validation of the angle of repose and seed ginger stacking behavior

Li et al. (2023) reported a measured angle of repose of 27.08°, which differed by 2.16° from the value of 29.24° obtained using the calibrated parameters in this study, corresponding to a relative error of 7.98%. This further supports the accuracy and reliability of the discrete element model of seed ginger and the calibrated parameters established in this study.

CONCLUSIONS

The key physical and mechanical properties of seed ginger during the sowing period were determined, and a discrete element model of seed ginger was constructed using the measured parameter values. The contact parameters between seed ginger and steel were calibrated, providing basic input parameters for simulation analysis of the seed-contacting components of ginger sowing machinery.

Using the angle of repose as the target response, a quadratic regression model relating the seed ginger–seed ginger contact parameters to the angle of repose was established through a steepest ascent test combined with Box–Behnken response surface methodology. The optimal parameter combination was obtained and validated by simulation. The relative error between the simulated and experimentally measured angles of repose was 2.24%, indicating that the established discrete element model of seed ginger has good accuracy and applicability.

The basic physical and mechanical properties and discrete element contact parameters of seed ginger with buds at the sowing stage were systematically measured. The calibration procedure for the contact parameters of irregularly shaped seed ginger was optimized. By combining the steepest ascent test with the response surface design, multiple contact parameters were optimized simultaneously, thereby improving calibration accuracy. The results provide reliable modeling support and a theoretical basis for the optimized design of key components of ginger sowing machinery, including single-seed selection and bud-orientation adjustment mechanisms.

ACKNOWLEDGEMENT

This study is funded by the National Key Research and Development Program (2024YFD2000403)

REFERENCES

[1] Cai, P., (2024). Design and simulation of vibratory yam harvesting machinery based on discrete element method (基于离散元法的振动式山药收获机械设计与仿真). *North China University of Water Resources and Electric Powe*r, Henan/China.

[2] Chen, T., Yi, S., Li, Y., (2023). Establishment of discrete element model and parameter calibration of alfalfa stem in budding stage (苜蓿现蕾期茎秆离散元模型建立与参数标定). *Transactions of the Chinese Society for Agricultural Machinery*, Vol. 54, pp. 91-100, Heilongjiang/China.

[3] Du, Z., Li, D., Li, X., (2025). Calibration and experiment of discrete element model parameters for tea stem (茶茎秆离散元模型参数标定与试验). *Transactions of the Chinese Society for Agricultural Machinery*, Vol. 56, pp. 311-320, Henan/China.

[4] Guo, H., Guo, L., Li, H., (2024). Calibration and experiment of the discrete element simulation parameters for rapeseed stems during the suitable harvest period (适收期油菜茎秆离散元仿真参数标定与试验). *Transactions of the Chinese Society of Agricultural Engineering*, Vol. 40, pp. 20-29, Xinjiang/China.

[5] Guo, H., Han, J., Lv, Z., (2025). Discrete element model construction and parameter calibration of combined harvest oil sunflower extract (联合收获油葵脱出物离散元模型构建与参数标定). *Transactions of the Chinese Society for Agricultural Machinery*, Vol. 56, pp. 319-330, Xinjiang/China.

[6] Huang Z., (2026). Determination of intrinsic parameters and DEM parameter calibration of multi-component particles in millet threshing mixtures(谷子脱出物多组分颗粒本征参数测定与离散元参数标定). *INMATEH - Agricultural Engineering*, Vol.78, Issue 1, pp. 656-672, Bucharest/Romania.

[7] Jiang, C., Du, X., Yang, Z., (2024). Analysis and experiment of punching and falling process for Auricularia heimuer fungal stick based on discrete element method (基于离散元的黑木耳菌棒刺孔与摆场下落过程分析与试验). *Transactions of the Chinese Society of Agricultural Engineering,* Vol. 40, pp. 30-38, Zhejiang/China.

[8] Jia S.L., (2021). Simulation analysis and construction of maize seeder model based on EDEM (EM solutions EDEM) (基于 EDEM 的玉米排种器模型构建与仿真分析). *INMATEH - Agricultural Engineering*, Vol.63, Issue 1, pp. 365-374, Bucharest/Romania.

[9] Liao, Y., Wang, Z., Liao, Q., (2020). Calibration of discrete element model parameters of forage rape stalk at early pod stage (果荚初期饲料油菜茎秆离散元接触模型参数标定). *Transactions of the Chinese Society for Agricultural Machinery*, Vol. 51, pp. 236-243, Wuhan/China.

[10] Lu, C., Gao, Z., Li, H., (2023). An ellipsoid modelling method for discrete element simulation of wheat seeds. *Biosystems Engineering*, Vol. 226, pp. 1-15, United Kingdom.

[11] Lu, Q., Liu, F., Liu, L., (2023). Establishment and verification of discrete element model for seed furrow soil-seed-soil covering device (种沟土壤-种子-覆土装置互作离散元模型建立与验证). *Transactions of the Chinese Society for Agricultural Machinery*, Vol. 54, pp. 46-57, Beijing/China.

[12] Liu F., (2020). Analysis and calibration of quinoa grain parameters used in a discrete element method based on the repose angle of the particle heap (基于堆积试验的藜麦离散元参数分析及标定). *INMATEH - Agricultural Engineering*, Vol.61, Issue 2, pp.77-86, Bucharest/Romania.

[13] Li, G., (2023). Development and experiment of suspended ginger combined seeder (悬挂式大姜联合播种机的研制与试验). *Shandong Agricultural University*, Shandong/China.

[14] Shi, L., Sun, W., Zhao, W., (2018). Parameter determination and validation of discrete element model of seed potato mechanical seeding (马铃薯种薯机械排种离散元仿真模型参数确定及验证). *Transactions of the Chinese Society of Agricultural Engineering*, Vol. 34, pp. 35-42, Gansu/China.

[15] Shi, R., Dai, F., Zhao, W., (2022). Establishment of discrete element flexible model and verification of contact parameters of flax stem (胡麻茎秆离散元柔性模型建立与接触参数试验验证). *Transactions of the Chinese Society for Agricultural Machinery*, Vol. 53, pp. 146-155, Gansu/China.

[16] Sun, K., Yu, J., Zhao, J., (2025). Parameter calibration and experimental validation of wheat straw model for cutting process simulation (面向切割过程仿真的小麦茎秆模型参数标定与试验验证). *Transactions of the Chinese Society for Agricultural Machinery*, Vol. 56, pp. 116-127, Jilin/China.

[17] Wang L., (2021). A general modelling approach for coated cotton-seeds based on the discrete element method (基于多目标优化的包衣棉种离散元接触参数标定). *INMATEH - Agricultural Engineering*, Vol.63, Issue 1, pp. 221-230, Bucharest/Romania.

[18] Xia, J., Zhang, P., Yuan, H., (2024). Calibration and verification of flexible rice straw model by discrete element method (水稻秸秆离散元柔性模型参数标定与试验验证). *Transactions of the Chinese Society for Agricultural Machinery*, Vol. 55, pp. 174-184, Wuhan/China.

[19] Xia, R., Li, B., Wang, X. W., (2019). Measurement and calibration of the discrete element parameters of wet bulk coal. *Measurement*, Vol. 142, pp. 84-95, Netherlands.

[20] Yang, K., (2022). Design and test of intelligent direction correction single-row ginger planter (自动调偏式单行大姜播种机的设计与试验). *Shandong Agricultural University*, Shandong/China.

[21] Yang J., (2026). Research on DEM calibration of contact parameters of sweet sorghum seed(甜高粱种子离散元接触参数标定研究). *INMATEH - Agricultural Engineering*, Vol.78, Issue 1, pp. 158-168, Bucharest/Romania.

[22] Zhang, G., Chen, L., Liu, H., (2022). Calibration and experiments of the discrete element simulation parameters for water chestnut (荸荠离散元仿真参数标定与试验). *Transactions of the Chinese Society of Agricultural Engineering*, Vol. 38, pp. 41-50, Wuhan/China.

[23] Zhang, H., (2025). Design and working parameter optimization of vibration conveying and separating device for sweet potato harvester (甘薯收获机振动输送分离装置设计及工作参数优化). *Shenyang Agricultural University*, Liaoning/China.

[24] Zhang, R., Zhou, J., Liu, H., (2022). Parameter calibration method of bonded corn particle model using discrete element method (玉米颗粒粘结模型离散元仿真参数标定方法研究). *Transactions of the Chinese Society for Agricultural Machinery*, Vol. 53, pp. 69-77, Shandong/China.

[25] Zhao, H., Wang, X., Zheng, Z., (2025). Research status and progress of discrete element method applications in agricultural equipment (农业装备领域离散元法应用研究进展). *Transactions of the Chinese Society for Agricultural Machinery*, Vol. 56, pp. 1-19, Shanxi/China.

[26] Zhou, J., (2023). Design and performance experimental study of potato picking device based on discrete element method (基于离散元法的马铃薯捡拾装置设计及其性能试验研究). *Inner Mongolia Agricultural University*, Inner Mongolia/China.